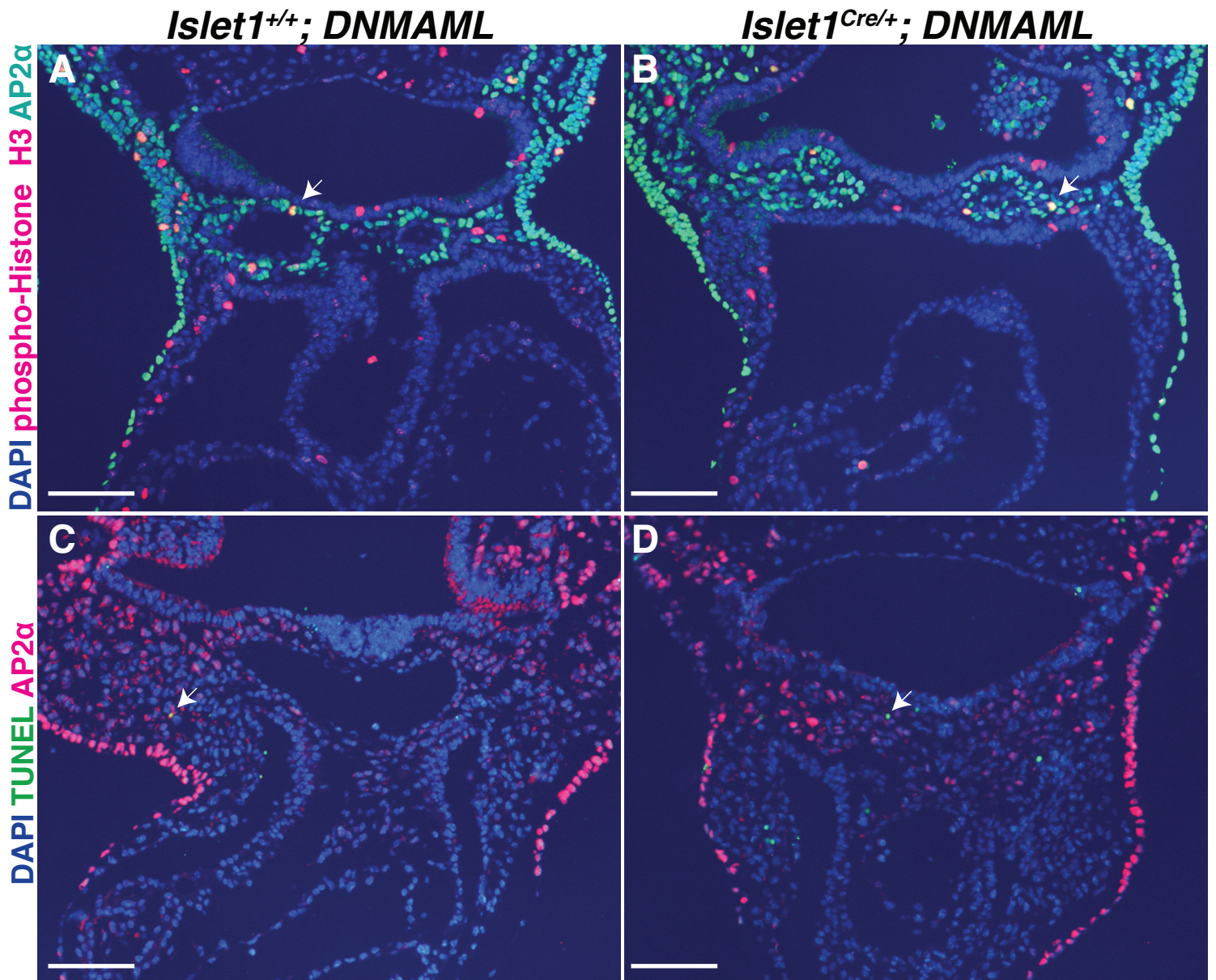
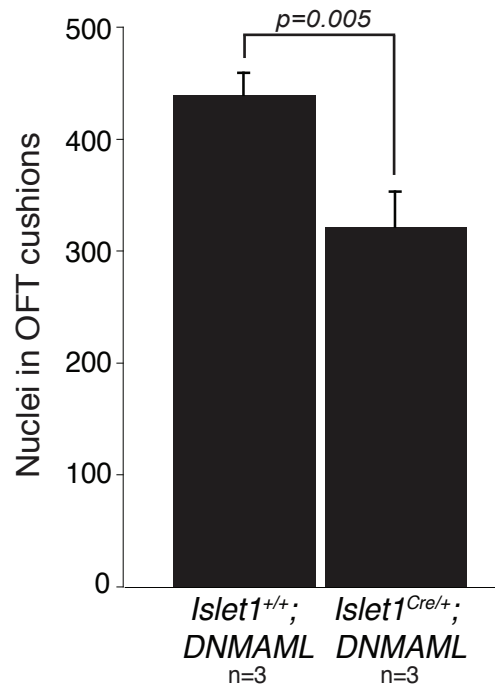


Supplementary Figure 1: Fate mapping of *Islet1Cre* and *Mef2c-AHF-Cre* derivatives. (A-D) Immunostaining for GFP to reveal DNMA1L-GFP expression in mutant embryos. (A and B) Comparable frontal sections through E12.5 *Islet1Cre/+; DNMA1L* (A) and *Mef2c-AHF-Cre +; DNMA1L* (B) embryos. Note that both Cre lines result in DNMA1L-GFP expression in the pharyngeal mesenchyme, while only *Islet1Cre/+; DNMA1L* embryos show DNMA1L-GFP expression in the pharyngeal endoderm. (C) Section through the aortic arch of an E17.5 *Islet1Cre/+; DNMA1L* embryo, showing DNMA1L-GFP expression in the second heart field-derived cells at the base of the truncus arteriosus (ta, arrowhead), while there is no significant contribution of DNMA1L-GFP positive cells to the aortic arch (ao). Note also DNMA1L-GFP expression in endoderm-derived tissues, including the esophagus and trachea. (D) Section through the heart of an E17.5 *Islet1Cre/+; DNMA1L* mutant, showing broad distribution of DNMA1L-GFP positive cells throughout the heart, including the right ventricle (rv), inter-ventricular septum (ivs), the majority of the left ventricle (lv), and regions of the right and left atria (ra, la). (E and F) Postnatal hearts from *Islet1Cre/+; R26RLacZ/+* (E) and *Mef2c-AHF-Cre +; R26RLacZ/+* (F) mice. Note that *Islet1Cre* results in Cre-mediated recombination throughout most of the heart, as well as the lungs and trachea. In contrast, *Mef2c-AHF-Cre* results in more restricted recombination in the right ventricle and OFT. Neither *Islet1Cre* nor *Mef2c-AHF-Cre* results in significant recombination in the aortic arch or its branches (arrowheads in E and F). Scale bars: 100 μ m (A-C), 250 μ m (D). Magnification: 30X (E) and 15X (F). Abbreviations: m: mesenchyme, e: pharyngeal endoderm, es: esophagus, tr: trachea, lu: lung, pa: pulmonary artery.

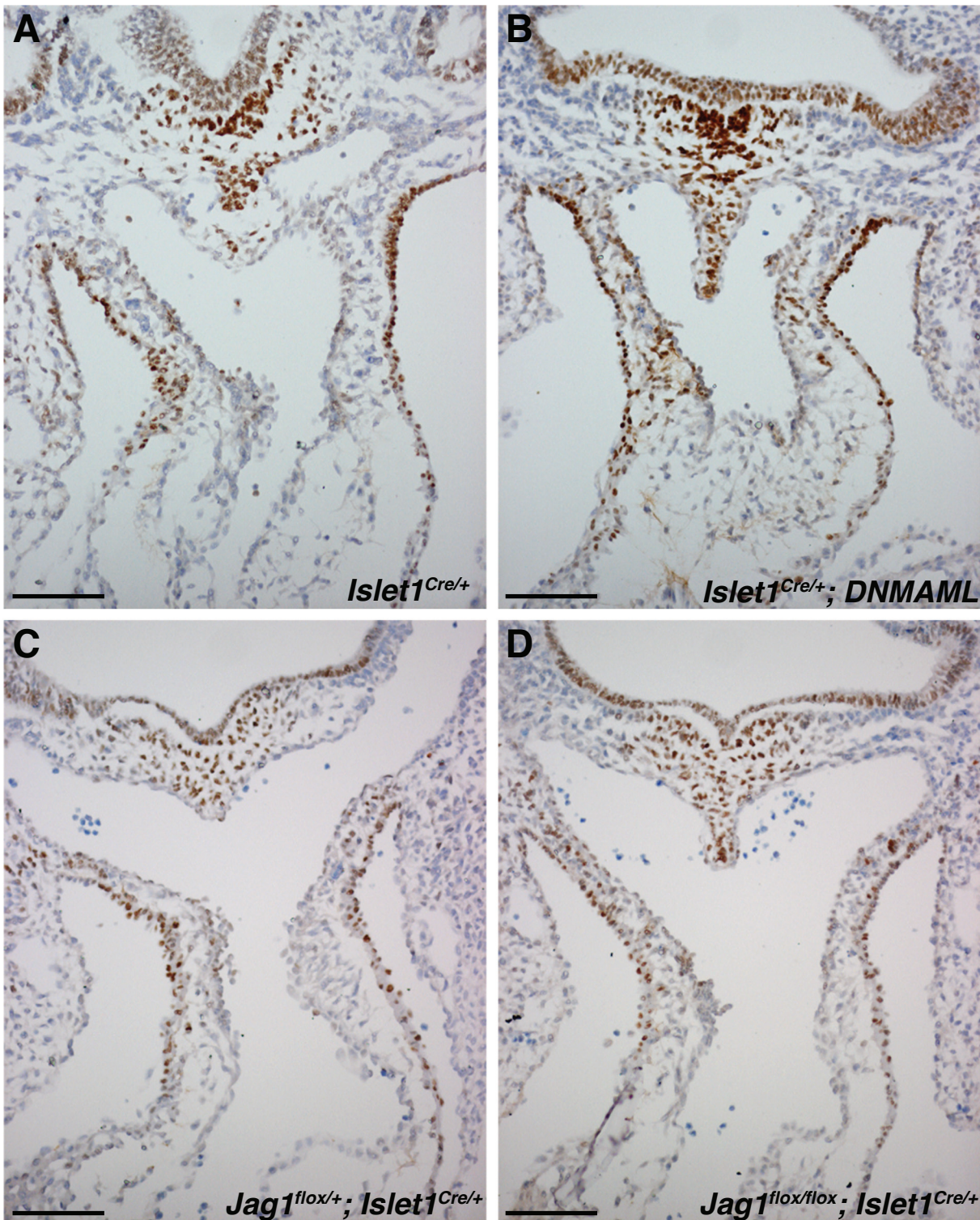


Supplementary Figure 2: Analysis of proliferation and apoptosis of neural crest.

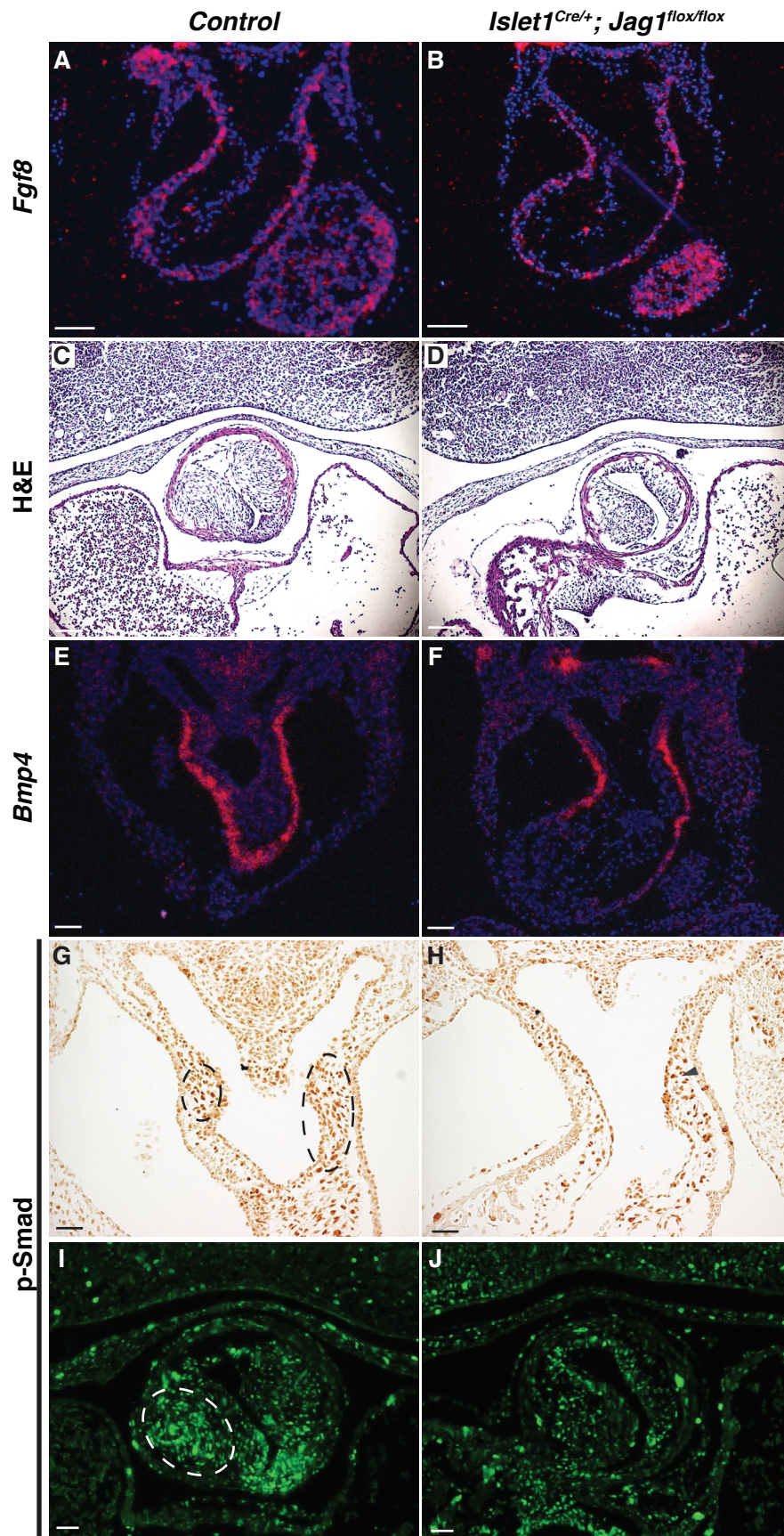
A, B - Costaining of Phospho-histone H3 (to show proliferation) and AP2α (a marker of neural crest and ectoderm) at E9.5. C,D - Costaining for TUNEL (to show apoptosis) and AP2α at E10. Arrows indicate co-stained cells. As discussed in the results section, no statistically significance was seen in the percentage of p-Histone3 positive or TUNEL positive neural crest cells between *Islet1*^{+/+}; DNMAML and *Islet1*^{Cre/+}; DNMAML in the ventral pharynx after analysis of serial sections of multiple litters. Scale bars: 100μm.



Supplementary Figure 2: Quantification of *Islet1*^{Cre/+}; DNMAML outflow tract cushion cells. Nuclei were counted in outflow tract cushions, both mutant and control, from 3 different E10.5 litters. There was a statistically significant difference in number of nuclei, $p=0.005$. Error bars represent one standard deviation.



Supplementary Figure 4: Islet1 Immunohistochemistry
(A and B) Representative cross sections of Islet1 IHC of *Islet1^{Cre/+}* (A) and *Islet1^{Cre/+}; DNMA1L* (B) embryos (E10.5). (C and D) Representative cross sections of *Jag1^{flox/+}; Islet1^{Cre/+}* (C) and *Jag1^{flox/flox}; Islet1^{Cre/+}* (D) littermates (E10). Quantitation of serial sections did not reveal a statistically significant difference in number of Islet1+ cells (see Results). Scale bars: 100µm.



Supplementary Figure 5: Cardiovascular defects and diminished *Fgf8* expression and *Bmp4* signaling in *Islet1^{Cre+}; Jag1^{flox/flox}* mutants. (A and B) In situ hybridizations for *Fgf8* on transverse sections of E9.5 control (A) and mutant (B) embryos. (C and D) Coronal H&E sections of E10.5 littermate embryos demonstrate normal OFT cushion cellularity in control embryos (C), but hypocellularity in the mutant OFT cushions (D). (E and F) In situ hybridization for *Bmp4* using transverse sections of control (E) and mutant (F) E10.5 embryos. (G-J) Phospho-Smad immunohistochemistry of E10.5 embryos of control (G and I) and mutants (H and J). Phospho-Smad positive cells are indicated by the dotted circle in I. Scale bars: 100 μ m.

Supplementary Table 1: Genotyping Data

Cross	Genotype	E9.5- E14.5	E17.5- E18.5	P0	P1- P7
<i>Islet1</i> ^{Cre/+} x <i>R26R</i> ^{DNMAML/DNMAML}	<i>R26R</i> ^{DNMAML/+}	127	11	3	18
	<i>Islet1</i> ^{Cre/+} ; <i>R26R</i> ^{DNMAML/+}	119	10	3*	0 ¹
<i>Mef2c-AHF-Cre</i> + x <i>R26R</i> ^{DNMAML/DNMAML}	<i>R26R</i> ^{DNMAML/+}	20	-	6	14
	<i>Mef2c-AHF-Cre</i> +; <i>R26R</i> ^{DNMAML/+}	16	-	9*	0 ²
<i>Islet1</i> ^{Cre/+} ; <i>Jag1</i> ^{fllox/+} x <i>Jag1</i> ^{fllox/flox}	<i>Jag1</i> ^{fllox/+}	33	21	4	-
	<i>Jag1</i> ^{fllox/flox}	40	24	8	-
	<i>Islet1</i> ^{Cre/+} ; <i>Jag1</i> ^{fllox/+}	28	25	9	-
	<i>Islet1</i> ^{Cre/+} ; <i>Jag1</i> ^{fllox/flox}	23	8	0 ³	-
<i>Mef2c-AHF-Cre</i> +; <i>Jag1</i> ^{fllox/+} x <i>Jag1</i> ^{fllox/flox}	<i>Jag1</i> ^{fllox/+}	2	2	13	-
	<i>Jag1</i> ^{fllox/flox}	2	6	7	-
	<i>Mef2c-AHF-Cre</i> +; <i>Jag1</i> ^{fllox/+}	3	1	15	-
	<i>Mef2c-AHF-Cre</i> +; <i>Jag1</i> ^{fllox/flox}	1	2	7*	-

¹p<0.0001; ²p=0.0002; ³p=0.01

* At P0 all mutants were dead or cyanotic